Molecular Dynamics Study of Bacteriorhodopsin and Artificial Pigments†

William Humphrey, Ilya Logunov, Klaus Schulten,* and Mordechai Sheves*,‡

Beckman Institute and Departments of Physics, Chemistry, and Biophysics, University of Illinois at Urbana-Champaign, 405 North Matthews, Urbana, Illinois 61801

Received October 4, 1993; Revised Manuscript Received January 5, 1994®

ABSTRACT: The structure of bacteriorhodopsin based on electron microscopy (EM) studies, as provided in Henderson *et al.* (1990), is refined using molecular dynamics simulations. The work is based on a previously refined and simulated structure which had added the interhelical loops to the EM model of bR. The present study applies an all-atom description to this structure and constraints to the original Henderson model, albeit with helix D shifted. Sixteen waters are then added to the protein, six in the retinal Schiff base region, four in the retinal–Asp-96 interstitial space, and six near the extracellular side. The root mean square deviation between the resulting structure and the Henderson et al. (1990) model measures only 1.8 Å. Further simulations of retinal analogues for substitutions at the 2- and 4-positions of retinal and an analogue without a β-ionone ring agree well with observed spectra. The resulting structure is characterized in view of bacteriorhodopsin's function; key features are (1) a retinal Schiff base–counterion complex which is formed by a hydrogen bridge network involving six water molecules, Asp-85, Asp-212, Tyr-185, Tyr-57, Arg-82, and Thr-89, and which exhibits Schiff base nitrogen–Asp-85 and –Asp-212 distances of 6 and 4.6 Å; (2) retinal assumes a corkscrew twist as one views retinal along its backbone; and (3) a deviation from the usual α-helical structure of the cytoplasmic side of helix G.

Bacteriorhodopsin (bR)[1] is a protein composed of seven α-helices which spans the purple membrane of *Halobacterium halobium* and which functions as a light-driven proton pump. It is a member of the retinal protein family, which contain a retinal chromophore bound within the protein interior via a protonated Schiff base linkage to Lys-216. For recent reviews, see Khorana (1988), Birge (1990), Mathies *et al.* (1991), Lanyi (1992), Oesterhelt *et al.* (1992), and Ebrey (1993).

Retinal in bR absorbs at 568 nm, while in methanol, a protonated retinal Schiff base absorbs at 440 nm. The spectral shift, known as the *opsin shift* (Nakanishi *et al.*, 1980), is attributed to electrostatic interactions which shift retinal's polyene-type electronic structure (absorbing around 400 nm) toward a polyenylic ion-type electronic structure (absorbing around 600 nm) (Schulten *et al.*, 1980) and to single bond torsions which disrupt the conjugation of retinal's π-electrons, thereby shifting the absorption to the blue. In a nonpolar solvent, the protonated Schiff base has a closely associated counterion, such as Cl^-, which shifts the electronic structure of retinal toward the polyene form, while in a polar solvent the Schiff base is strongly hydrogen-bonded to solvent dipoles which shield the interactions with the negative ion and shift retinal's structure toward the polyenylic ion form. In bR_{568}, it is suggested that the protonated Schiff base linkage experiences hydrogen-bonding as well as electrostatic interactions with the negatively charged neighboring Asp-85 and Asp-212 side groups, with both interactions affecting retinal's absorption spectrum. Furthermore, in bR_{568} the spectrum is shifted through a torsion of retinal's β-ionone ring. In solution, the ring is in a twisted 6-s-*cis* conformation which blue-shifts the spectrum, whereas in bR_{568} a planar 6-s-*trans* conformation prevails which leads to a maximum absorption wavelength. The overall effect of electrostatic and sterical interactions is a strong red shift, namely, the 440 nm → 568 nm opsin shift (Harbison *et al.*, 1985; van der Steen *et al.*, 1986).

Bacteriorhodopsin transfers protons from the cytoplasmic to the extracellular side of the membrane through a cyclic process initiated by absorption of a photon. This photon triggers an isomerization of retinal, which proceeds then through several intermediate states identified by their absorption spectra. An accepted kinetic scheme for this cycle is an unbranched series of intermediates:

$$bR_{568} \rightarrow J_{625} \leftrightarrow K_{590} \leftrightarrow L_{550} \leftrightarrow M_{412} \leftrightarrow N_{520} \leftrightarrow O_{640} \leftrightarrow bR_{568}$$

where the indices denote the absorption maxima of the respective intermediates. Photoisomerization occurs in the $bR_{568} \rightarrow J_{625}$ transition. During the $L_{550} \rightarrow M_{412}$ transition the Schiff base proton is transferred to Asp-85 and, subsequently, to the outside of the cell (Schulten & Tavan, 1978; Mogi *et al.*, 1989a,b; Braiman *et al.*, 1988; Stern & Khorana, 1989; Gerwert *et al.*, 1989). During the $M_{412} \rightarrow N_{520}$ transition, a proton is transferred to the Schiff base from Asp-96, which then takes up a proton from the cytoplasmic environment (Gerwert *et al.*, 1989). The reaction cycle is completed as the protein returns to bR_{568} in the final transitions.

Several researchers have proposed that the $L_{550} \leftrightarrow M_{412} \leftrightarrow N_{520}$ transitions involve actually two M forms, $M_{(I)}$ and $M_{(II)}$ (Dancshazy *et al.*, 1988; Kouyama *et al.*, 1988; Lozier *et al.*, 1978; Nagle & Mille, 1981; Schulten *et al.*, 1984; Gerwert & Siebert, 1986; Renard & Delmelle, 1985). Detailed models were suggested by Orlandi and Schulten (1979) and Váró & Lanyi (1990, 1991a,b), who suggested that the $M_{(I)} \rightarrow M_{(II)}$ transition is attributed to a switch of the protonation site of the retinal Schiff base from an extracellular to a cytoplasmic proton pathway.

Several studies have suggested the presence of water molecules within bacteriorhodopsin. The involvement of water in stabilizing the protonated Schiff base was suggested by

† This work was supported by a grant from the National Institutes of Health (P41RR05969).

* To whom correspondence should be addressed.

‡ Permanent address: Department of Organic Chemistry, The Weizmann Institute of Science, Rehovot 76100, Israel.

® Abstract published in *Advance ACS Abstracts,* February 15, 1994.

[1] Abbreviations: bR, bacteriorhodopsin; CD, circular dichroism; FTIR, Fourier transform infrared; NMR, nuclear magnetic resonance; RMS(D), root mean square (deviation).

0006-2960/94/0433-3668$04.50/0

Dupuis *et al.* (1980), by Hildebrandt and Stockburger (1984) on the basis of resonance Raman studies of dried membrane, and by de Groot *et al.* (1989) on the basis of ^{15}N NMR studies. Neutron diffraction data have indicated at least 11 water molecules within the interior of bR, with four located near the Schiff base binding site (Papadopolous *et al.*, 1990). Recently it was suggested (Gat & Sheves, 1993) that in bR a specific orientation between the Schiff base and carboxyl groups allows water molecules to form a well-defined structure which bridges the charged groups. This structure stabilizes the ion pair (protonated Schiff base/counterion) and leads to the unusually high pK_a value of the protonated Schiff base and low pK_a of the aspartic acids. In addition, water molecules have also been suggested to participate in the transfer of the proton from Asp-96 to the Schiff base (Henderson *et al.*, 1990; Váró & Lanyi, 1990). Water is also expected to contribute significantly to the pK_a values of relevant titratable groups in bR (B. Honig, private communication). Observed changes in the water structure during the photocycle (Maeda *et al.*, 1992) and changes in the absorption maximum of bR_{568} upon dehydration (Hildebrandt & Stockburger, 1984; Papadopolous *et al.*, 1990; Renthal & Regalado, 1991) support an important role of water in bR. The participation of water and amino acid side groups in proton transport in bR has been discussed also in Brünger *et al.* (1983).

The publication of the structure of bacteriorhodopsin by Henderson *et al.* (1990) based on electron microscopy studies has been a seminal event for research on retinal proteins. Unfortunately, the structure does not yet resolve sufficient detail to explain the mechanism of proton pumping in bR. For example, the structure determined by Henderson *et al.* (1990) resolves only the membrane-spanning residues of the seven α-helices of bR but not the interhelical loops. These loops had been added and the structure had been refined in a previous molecular dynamics study of bR by Nonella *et al.* (1991). The EM structure also does not resolve any of the water molecules inside bacteriorhodopsin. A first attempt to place water into a simulated bacteriorhodopsin molecule and to further refine its structure had been made by Zhou *et al.* (1993).

In this paper, we extend the work of previous molecular dynamics studies of bR (Nonella *et al.*, 1991; Zhou *et al.*, 1993) and further refine the structure for bR_{568} by means of molecular dynamics simulations, focusing mainly on the retinal binding site. The previous refinements were improved in several respects. First, we incorporated into the simulations new data by Henderson *et al.* (R. Henderson, private communication), which shift the D helix 3 Å toward the cytoplasmic side of bR. Second, we changed significantly the refinement protocol of the earlier studies (Nonella *et al.*, 1991; Zhou *et al.*, 1993): after addition of the loops and of sixteen water molecules, the structure was constrained back to the EM structure coordinates of the transmembrane segment. Third, we employed observations on bacteriorhodopsin reconstituted with retinal analogues [see for a review Ottolenghi and Sheves (1989)] as tests of our structure. In doing so we realized that combined atom simulations, *e.g.*, representations of CH_2 moieties by effective single atoms, are not sufficient to account for sterical interactions of retinal with its binding site. Therefore, we adopted as a fourth improvement an all-atom description for the refinement.

Below we will first summarize under Experimental Procedures the simulation protocol employed for the refinement and for molecular dynamics calculations which test the properties of the resulting structure. We then describe under Results the simulated structure of native bacteriorhodopsin and its changes upon replacement of retinal by various retinal analogues. We then appraise under Discussion the proposed structure obtained in the light of a large number of observations and discuss, finally, under Conclusions the implications of the refined structure for the proton pump mechanism of bacteriorhodopsin. The structure of bR_{568} obtained in this study will be made available upon request.

EXPERIMENTAL PROCEDURES

The original structure of bR, as determined by Henderson *et al.* (1990), resolved the membrane-spanning helical residues; the turns had been added to this structure and equilibrated by molecular dynamics simulations in Nonella *et al.* (1991). The backbone atoms of the resulting structure had an RMSD of 2.8 Å as compared to the Henderson structure. Our refinement employed the structure in Nonella *et al.* (1991) as a starting point. The program X-PLOR (Brünger, 1988), which uses the CHARMm energy function (Brooks *et al.*, 1983), was used for all molecular dynamics simulations. All simulations were carried out at a temperature of 300 K and employed a cutoff distance of 8 Å and a dielectric constant of $\epsilon = 1$ for the evaluation of Coulomb interactions.

Both the structure proposed by Henderson *et al.* (1990) and that refined in Nonella *et al.* (1991) do not specify hydrogen atoms explicitly, except for the protein backbone and for protonated amino acids. In the present study, all atoms are described explicitly. We also employ an explicit hydrogen-bonding term in the energy function. The all atom representation was obtained by adding hydrogens to the structure in Nonella *et al.* (1991) using the HBUILD command of X-PLOR. The parameters and charges used in the simulations are, respectively, the parmallh3x.pro parameters and topallh6x.pro charges (Brooks *et al.*, 1983; Brünger, 1988), except for retinal.

The charges employed for the protonated Schiff base of retinal in bR are those reported in Nonella *et al.* (1991), and used in Zhou *et al.* (1993), with slight modifications. The original charges were chosen for the united atom model; the explicit hydrogens added to the retinal backbone were given partial charges of 0.03, with the corresponding heavy atom charges reduced by 0.03 to preserve net charge. The charges assumed in Nonella *et al.* (1991) and Zhou *et al.* (1993) for the Schiff base nitrogen and proton were –0.509 and 0.519, respectively; however, quantum chemical calculations of retinal charge distributions (Tavan *et al.*, 1985; Birge *et al.*, 1987; Carlacci *et al.*, 1991) have indicated that these charges might be too large. In our simulations, we have reduced the charges on these atoms to –0.309 and 0.319 for the Schiff base nitrogen and proton, respectively. It is not clear yet if this is the best choice. In a recent extensive quantum chemical calculation of a retinal Schiff base fragment, Nina and Smith determined the respective charges as –0.727 and 0.505 (Nina and Smith, manuscript in preparation).

Equilibrium bond lengths, angles, and torsional angles for retinal are those determined by recent X-ray crystallography studies (Santasiero and James, 1990). The retinal geometry in bR_{568} is all-*trans*. Force constants for retinal are derived from molecules with similar chemical structures for which parameters are available in CHARMm and X-PLOR. Retinal backbone single- and double-bond torsional barriers are given in Table 1. Barriers for the backbone single bonds are 5 kcal/mol, and for the double bonds, 30 kcal/mol, with the exception of the bonds in the vicinity of the Schiff base. The C_{13}–C_{14} and C_{15}–N_{SB} double-bond barriers are reduced to 20 kcal/

Table 1: Retinal Backbone Torsional Barriers k_{ϕ_i} in the Torsional Potentials $E_i^{dihe} = {}^1/_2 k_{\phi_i}[1 + \cos(2\phi_i + \delta_i)]$

ϕ_i	k_{ϕ_i} (kcal/mol)	ϕ_i	k_{ϕ_i} (kcal/mol)
C_5–C_6–C_7–C_8	5.0	C_6–C_7–C_8–C_9	30.0
C_7–C_8–C_9–C_{10}	5.0	C_8–C_9–C_{10}–C_{11}	30.0
C_9–C_{10}–C_{11}–C_{12}	5.0	C_{10}–C_{11}–C_{12}–C_{13}	30.0
C_{11}–C_{12}–C_{13}–C_{14}	5.0	C_{12}–C_{13}–C_{14}–C_{15}	20.0
C_{13}–C_{14}–C_{15}–N_{SB}	10.0	C_{14}–C_{15}–N_{SB}–C_ϵ	20.0

mol, and the C_{14}–C_{15} single-bond barrier is increased to 10 kcal/mol, in keeping with quantum chemical calculations in Schulten and Tavan (1978) and Schulten *et al.* (1984).

The protonation states of titratable groups in bR are as given in the standard X-PLOR amino acid topology files, except for Asp-96 and Asp-115, which are assumed to be protonated according to the observations in Gerwert *et al.* (1989) and Engelhard *et al.* (1990). As suggested previously (Bashford & Gerwert, 1992; Zhou *et al.*, 1993), Arg-82 has been moved up to a position facing toward the cytoplasmic side of the protein. In this position, Arg-82 is part of the Schiff base–counterion complex.

In the original structure proposed by Henderson *et al.* (1990), helix D was the least resolved segment of the seven α-helix protein, because it does not contain any bulky aromatic side chains. By incorporation of many more experimental observations, it has since been discovered that this helix should be positioned 3 Å toward the cytoplasmic side of bR (R. Henderson, private communication). To achieve this in our simulated structure, we modified the original coordinates of the EM model of bR by moving helix D using the molecular graphics program Quanta (Polygen, 1988) and harmonically constrained the C_α atoms of all seven helices in the starting structure to the corresponding shifted EM coordinates. These constraints were applied for 30 ps, followed by 10 ps of equilibration and energy minimization.

After these calculations, 16 water molecules were placed within the interior of bR, in three regions: above the Schiff base toward the cytoplasmic side, around the Schiff base, and below the Schiff base toward the extracellular side. These water molecules are described according to the TIP3P water model (Jorgenson *et al.*, 1983). Six water molecules were placed in the region proximate to the Schiff base, four were placed above the Schiff base in the region proximate to Asp-96, and six were placed below the counterion in the region close to the extracellular side. After the placement of water, the system was equilibrated for 20 ps and energy-minimized. The resulting structure has been further simulated for 30 ps to test the stability of the structure and determine various properties, e.g., RMSD values.

Retinal modifications were performed on the final bR_{568} structure. The modifications were accomplished with the PATCH facility of X-PLOR; initial coordinates were assigned using the positions of replaced atoms and using the HBUILD command to generate coordinates for explicitly added hydrogens. For all simulations, including retinal analogues, we carried out energy minimization after the modifications, followed by 5 ps of equilibration and 5 ps of dynamics, and further energy minimization. Table 2 lists the partial charges used in our simulations of retinal analogues.

RESULTS

This section provides a description of the molecular dynamics simulations carried out and characterizes the resulting structures. The relationship of the structural characteristics to observations is the subject of the Discussion section.

Table 2: Partial Charges for Retinal Analogues

4-dimethylamino				4-methyl and 2-methyl	
N_4	–0.060				
C_{21}	0.030	C_{22}	0.030	C_{21}	–0.040
H_{21A}	0.000	H_{22A}	0.000	H_{21A}	0.000
H_{21B}	0.000	H_{22B}	0.000	H_{21B}	0.000
H_{21C}	0.000	H_{22C}	0.000	H_{21C}	0.000

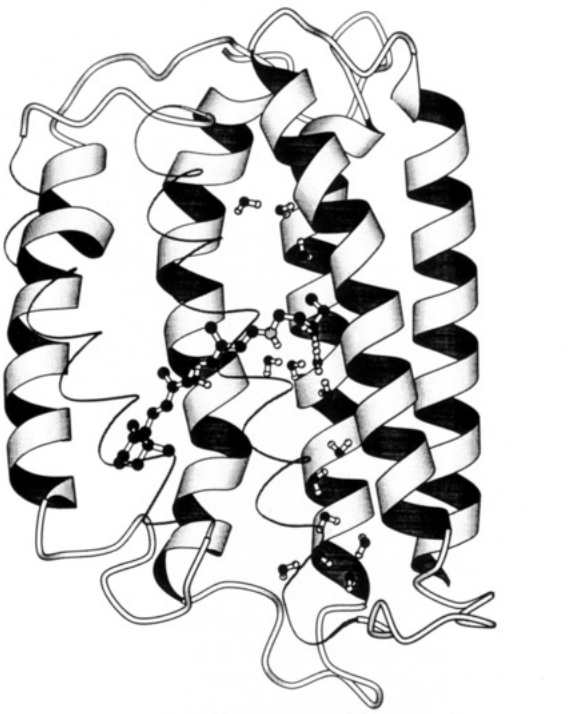

FIGURE 1: Ribbon diagram of bR, including retinal and water molecules, generated with MOLSCRIPT (Kraulis, 1991). Helices C and D are shown as thin lines to reveal the protein interior.

Construction of bR_{568}. Following the addition of explicit hydrogens to the structure proposed by Nonella *et al.* (1991), simulation G1 constrained the C_α atoms of this structure to the corresponding atoms in the structure of Henderson *et al.* (1990), with helix D shifted 3 Å toward the cytoplasmic side of the membrane, as described in Experimental Procedures. The resulting structure had an RMSD of 1.8 Å for the backbone C_α atoms as compared to the shifted Henderson *et al.* (1990) structure, a value much improved compared to the 2.8-Å RMSD for the structure as proposed by Nonella *et al.* (1991). For helix D, the RMSD was 2.3 Å, which is larger than the total RMSD but still reduced compared to the earlier value of 2.8 Å.

Following simulation G1, water molecules were added to the simulated structure as described in Experimental Procedures. In simulation G2, this system was equilibrated for 20 ps, followed by final energy minimization. The resulting proposed structure, labeled bR_{568}, is presented in Figures 1–5. Figure 1 shows the protein backbone, water, and retinal, as well as the added loop regions. The retinal long axis is at an angle of about 30° to the plane of the membrane, somewhat larger but still consistent with measured angles of 20° ± 10°. The methyls at C_9 and C_{13} remain pointing to the cytoplasmic side (Heyn *et al.*, 1988; Earnest *et al.*, 1986; Lin and Mathies, 1989; Henderson *et al.*, 1990). In the vicinity of the retinal ring, the average tilt of the retinal long axis is somewhat larger than the average tilt of retinal as a whole, by about 10°, due to a slight curvature in the retinal backbone.

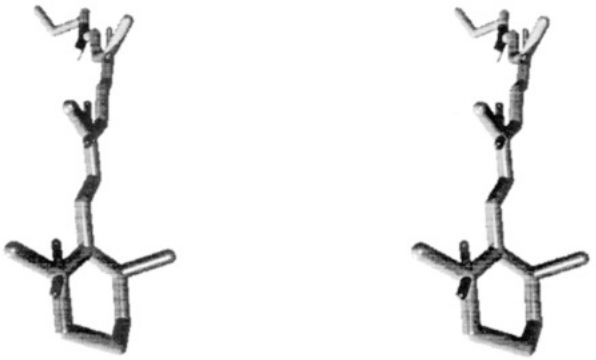

FIGURE 2: Stereo diagram of retinal's twisted configuration. Thin dark cylinders originating from the C_5, C_9, and C_{13} positions indicate axes used to measure the orientation of methyl groups (Table 3).

Table 3: Twist Angles for Retinal Methyl Groups[a]

methyl	ϕ	θ_{sim}	θ_{exp} (±1°)
C_{18}	−64.7	48.6	37
C_{19}	−27.8	41.4	40
C_{20}	57.8	34.5	32

[a] Values for θ_{exp} were determined by solid-state ^{2}H-NMR studies (Ulrich *et al.*, 1992; Ulrich, Watts, Wallat, and Heyn, private communication).

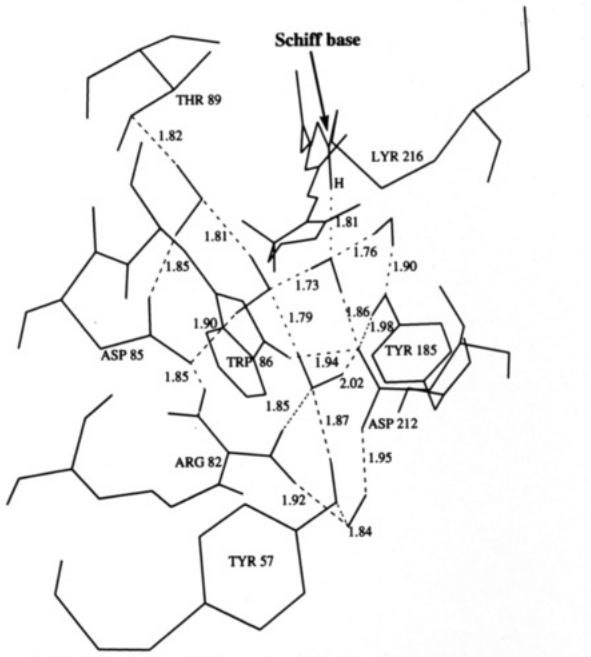

FIGURE 3: Detailed view of the retinal binding site, showing positions of water molecules and important residues and distances of possible hydrogen bonds.

An interesting feature of the proposed bR_{568} structure is a distinctive twist of retinal's backbone, as shown in Figure 2. Obviously, retinal is not planar in this structure; instead it displays a "corkscrew" configuration, as one views retinal along its backbone. This twist is a result of torsions around retinal's single bonds, especially around the C_5–C_6, C_{10}–C_{11}, and C_{12}–C_{13} bonds by 15°, 15°, and 30°, respectively. In Figure 2, thin cylinders originating from the C_5, C_9, and C_{13} atoms indicate axes used to determine orientation angles for the methyl groups at these positions. The vertical cylinders, representing the z axis, are parallel to the membrane normal. The horizontal (out of the page) axes, representing the x axis, are orthogonal to the z axis and in the plane formed by the membrane normal and the average direction of the retinal backbone. Table 3 lists the angles which define the orientation of the retinal backbone methyl groups. The angle θ measures the tilt from the z axis, and the angle ϕ measures the orientation of this tilt from the x axis. Also listed in Table 3 are measured values for θ determined by solid-state ^{2}H-NMR studies (Ulrich *et al.*, 1992; M. Heyn, private communication).

A detailed picture of the Schiff base region is given in Figure 3, which shows the relative positions of active groups in the binding site, as well as the positions and orientations of water molecules in this region. Possible hydrogen bonds are shown as dashed lines accompanied by the associated distances from hydrogen to hydrogen-bond acceptor. An interesting feature of this structure is associated with a hydrogen-bonding network within the binding site involving water molecules and protein residues. Within the immediate Schiff base linkage vicinity, there are four water molecules; two additional water molecules are in close proximity. The water molecules most proximate to the Schiff base all have three of four hydrogen-bonding partners. The Schiff base is hydrogen-bonded to only one water molecule; this hydrogen bond differs from a linear conformation by 31°, in keeping with resonance Raman and FTIR spectra which suggest that weak hydrogen bonding prevails between the protonated Schiff base linkage and its environment (Aton *et al.*, 1980; Kakitani *et al.*, 1983; Baasov *et al.*, 1987).

In the simulated structure, both oxygens of the Asp-85 carboxylate are located at a distance of 6 Å from the Schiff base. One oxygen of the Asp-212 carboxylate is located at a distance of 4.6 Å from the Schiff base, the other at a distance of 6.5 Å. Asp-85 has two water molecules hydrogen-bonded to the carboxylate, which is also bound to Arg-82. There is no direct interaction of the Schiff base with Asp-85, the two groups being bridged by two water molecules. While Asp-212 is located closer to the Schiff base than Asp-85, it also is connected to retinal only indirectly through one water molecule. Figure 3 shows that there are up to four groups within hydrogen-bonding distance of the carboxylate oxygen of Asp-212 closest to the Schiff base, shielding it from the Schiff base charge. While it is not feasible for all these groups to hydrogen-bond to the same oxygen of Asp-212, their proximity does provide an effective screen for the carboxyl group. A water molecule is hydrogen-bonded to the other oxygen of the Asp-212 carboxylate; this water molecule is also hydrogen-bonded to Tyr-57 and Arg-82.

Tyr-57 is hydrogen-bonded to two water molecules in this suggested structure: one of the waters is hydrogen-bonded to Arg-82, to another water molecule, and possibly to Asp-212 as well; the other water is hydrogen-bonded to Arg-82 and possibly to Asp-212. Tyr-185 is within hydrogen-bonding distance of Asp-212, as well as being hydrogen-bonded to one water molecule which is bound to the water molecule near the Schiff base. Both tyrosine residues have their hydroxyl groups oriented toward the Schiff base environment, but they are separated enough from the Schiff base to preclude any direct interaction: Tyr-57 is separated by 6.9 Å from the Schiff base, and Tyr-185 by 4.6 Å. Arg-82 has been directed in our simulated bR_{568} structure toward the Schiff base and remained in this position throughout all refinement steps, hydrogen-bonding directly to Asp-85 and, indirectly, to Asp-212 and to Tyr-57 via water molecules. Trp-86 seems to participate in the least number of hydrogen bonds, the only candidate being a possible bond with Asp-212. Trp-86 serves the role of maintaining a boundary for the hydrophilic region around the Schiff base. Thr-89 also participates in the hydrogen-bonded network described, with its hydroxyl group hydrogen-bonded to a water molecule which is also hydrogen-bonded to Asp-85.

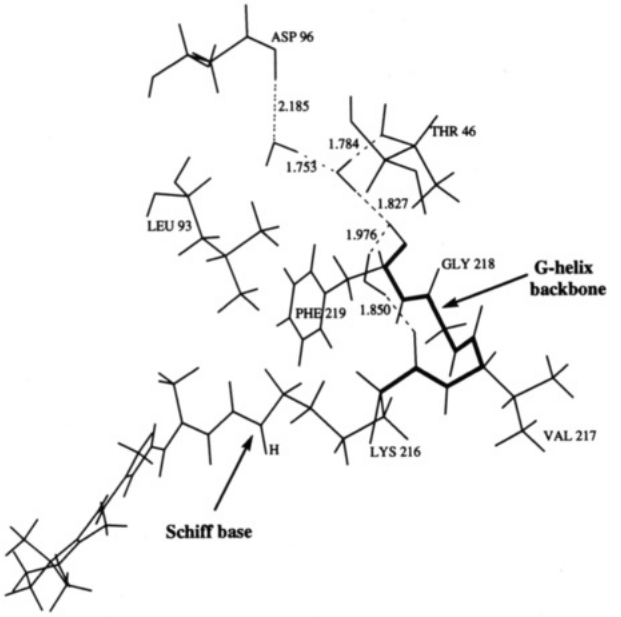

FIGURE 4: View of the region above the Schiff base, toward the cytoplasmic side of the membrane.

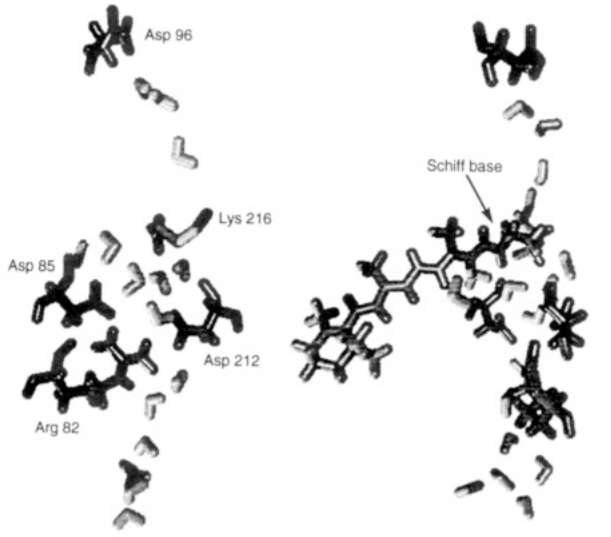

FIGURE 5: Solid model images of retinal and key groups near and above the binding site region, from two different perspectives. The left image shows only a portion of retinal for clarity.

Above the Schiff base, toward the cytoplasmic side of the membrane, helix G exhibits an unusual conformation. Figure 4 provides a detailed view of this region, indicating possible hydrogen bonds by dashed lines. The simulated structure contains three water molecules between the protonated Asp-96 and the Lys-216 to which retinal is attached. These water molecules, along with Phe-219, form a hydrogen-bonded chain between Asp-96 and the carbonyl of Lys-216. The helix G backbone along this chain is seen to be distorted from a standard α-helical conformation, with the carbonyl of Phe-219 oriented perpendicular to the helix instead of parallel. This carbonyl is hydrogen-bonded to two water molecules, which breaks the standard hydrogen bond between the CO group of Phe-219 and the NH group of Leu-223. One of these water molecules is hydrogen-bonded to the carbonyl of Lys-216, forming a weak hydrogen bond due to a 60° angle between the hydrogen–donor pair and the acceptor–antecedent pair. The other water molecule is hydrogen-bonded to Thr-46 and also to a third water molecule which hydrogen-bonds

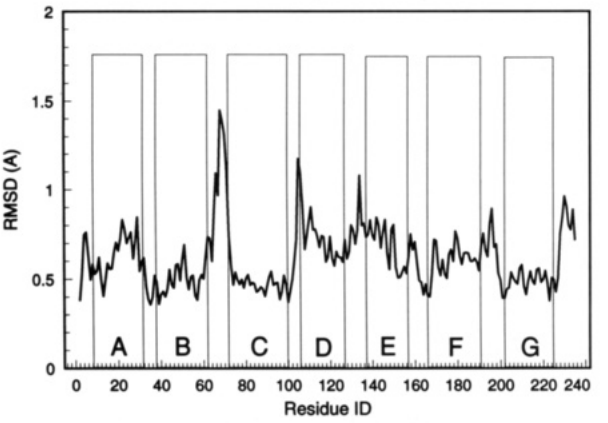

FIGURE 6: RMS deviations for C_α atoms resulting from simulation G3. Boxed regions A–G indicate the α-helical segments of bR.

to Asp-96. This chain provides an indirect interaction between Thr-46 and Asp-96.

To test if the distortion in helix G is a result arising from the particular placement of water molecules used here, two simulations were done, each starting from the refined bR_{568} structure and running for 25 ps. In the first simulation, the two water molecules hydrogen-bonded to helix G above the Schiff base vicinity were removed. During this time, the helix maintained the distortion from an α-helical form, with the water molecule originally hydrogen-bonded to Asp-96 moving to form a hydrogen bond with Phe-219, reinstating the hydrogen bond lost when the water molecules were removed. In the second, all three water molecules placed in the region between the Schiff base and Asp-96 were removed. Within the 25 ps simulated, the helix remained in the distorted form, but it is possible that the helix could return to a standard α-helical state given more time.

NMR spectroscopy may be able to reveal the distance from the C_{19} atom of retinal to the closest tryptophan residue (J. Herzfeld, private communication). In our bR_{568} structure, with retinal oriented with its methyl groups at the C_5, C_9, and C_{13} positions toward the cytoplasmic side of the membrane, the closest tryptophan residue is Trp-182, located 3.7 Å from C_{19}. In the Henderson *et al.* (1990) structure, with retinal oriented in the same manner, this distance is 3.4 Å.

Stability of bR_{568}. To test the stability of the described bR_{568} structure, we carried out simulation G3, which lasted 30 ps. Figures 6 and 7 summarize the results of this simulation. In Figure 6, the RMSD of the C_α atoms is shown, with the seven α-helices A–G indicated by boxed regions. The turn regions exhibit the largest deviations, while helices B, C, and G show small deviations, of 0.4–0.5 Å. For all the helical portions except helix D, the RMSD is less than 0.8 Å, while for helix D the residues close to the cytoplasmic side show higher RMSDs. Helix D is expected to have a somewhat larger mobility, since it is one of the smallest helices in bR and does not contain any bulky residues.

Figure 7 shows the suggested distances of the carboxylate oxygens of residues Asp-85 and Asp-212 to the Schiff base proton, as well as the RMSD of the C_α atoms relative to bR_{568}, during simulation G3. Asp-212 is seen to remain rather immobile, with distance values of 4.6 and 6.5 Å for the two oxygens. Asp-85 exhibits larger fluctuations, but its motion is still relatively small, with both oxygens maintaining a distance of about 5.8 Å. The RMSD of the C_α atoms fluctuates slightly during the simulation, mostly staying in the region of 0.8–1.2 Å. Following an initial relaxation of about 5 ps, where the RMSD increases to around 0.8 Å, the RMSD remains

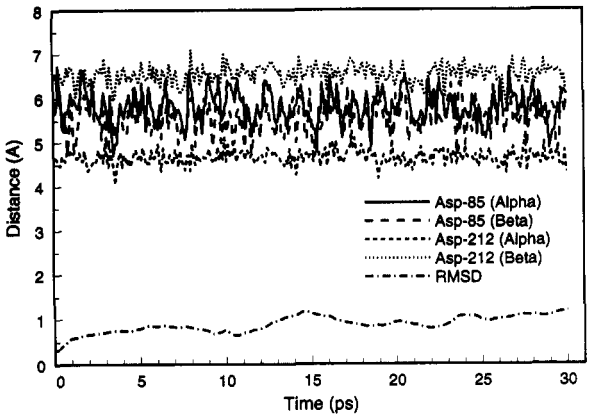

FIGURE 7: Distances of oxygen atoms in the carboxylates of Asp-85 and Asp-212 to the Schiff base proton and RMS deviations of C_α atoms from bR_{568}, during simulation G3.

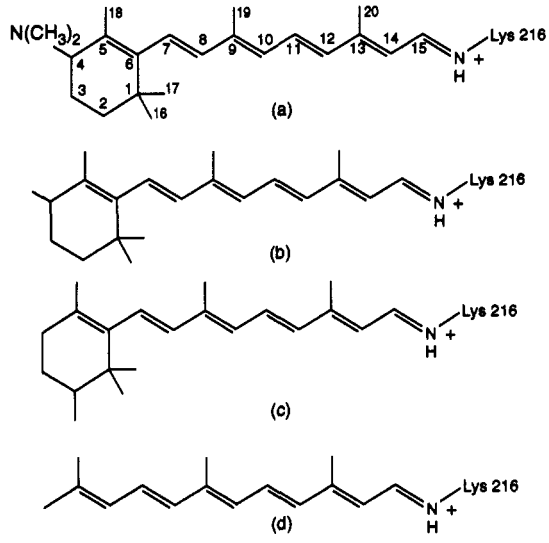

FIGURE 8: Retinal analogues: (a) 4-Dimethylamino analogue and numbering scheme of retinal atoms; (b) 4-methyl analogue; (c) 2-methyl analogue; (d) cleaved-ring analogue.

close to an average value of 1.0 Å. The immobility of residues Asp-85 and Asp-212 and the relatively small RMSD of the protein provides a good indication of the stability of retinal's counterion complex and overall structure.

Retinal Analogue Simulations. Experiments with modified retinal chromophores have provided useful information on the behavior of retinal within the binding site and on the surrounding environment (Ottolenghi & Sheves, 1989). In this study we focus on modifications to the β-ionone ring region of retinal, which provide clues about the orientation and location of the retinal ring within the binding site. Figure 8 illustrates the analogues considered here. It was observed that introduction of bulky substituents at the ring C_4 position blue-shifted the absorption maximum of bR considerably (Sheves *et al.*, 1984). In contrast, substitution at the C_2 position with a methyl group did not cause any significant change in the absorption maximum (Sheves and Friedman, unpublished results). Simulations of these artificial pigments, related to the spectral shifts observed for the respective pigments, should provide a measure of the consistency and accuracy of the refinement suggested in this study. Results for these simulations are given in Figures 9 and 10.

(A) 4-Dimethylamino Modification. Simulations R1A and R1B were carried out to determine the effect of the addition of a dimethylamino group to the C_4 position of retinal and

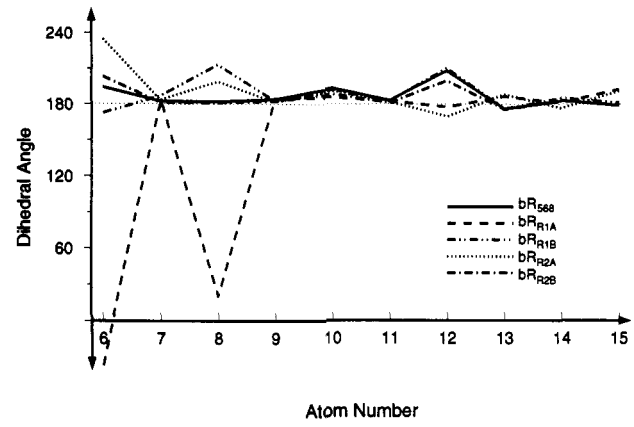

FIGURE 9: Comparison of dihedral angles along retinal backbone, for substitutions at the C_4 position; the numbering scheme is defined in Figure 8.

resulted in two structures, bR_{R1A} and bR_{R1B}. The C_4 position has two hydrogen atoms bound to the carbon; thus, there are two possibilities for attachment of the dimethylamino group. We define the plane of retinal facing toward the extracellular side as α and that facing to the cytoplasmic side as β. Simulation R1A models substitution at the α-position, R1B at the β-position.

Figure 9 summarizes the results of both simulations. Shown in this figure are the torsional angles of bonds along the retinal backbone. For the native pigment, all retinal backbone bonds are in the s-*trans* configuration, with the C_6–C_7, C_{10}–C_{11}, and C_{12}–C_{13} bonds slightly twisted, giving rise to the corkscrew configuration of retinal in bR_{568} discussed above. In our simulations the changes of retinal's conformation in going from bR_{568} to bR_{R1A} are quite dramatic. The C_6–C_7 and C_8–C_9 bonds rotate from an s-*trans* to an s-*cis* conformation, while the C_{12}–C_{13} bond relaxes completely to the s-*trans* state. Both the C_6–C_7 and the C_8–C_9 bond twist by about 30° from planar s-*cis* conformations. In the case of bR_{R1B}, the resulting conformation shows some change relative to bR_{568}, but all retinal backbone bonds remain in the s-*trans* conformation. The main changes detected in the molecular dynamics simulations are in the C_6–C_7 and C_8–C_9 torsional angles. The rotation about the C_6–C_7 bond measures about 20°, reducing the 30° twist angle of native retinal. The rotation about the C_8–C_9 bond, however, measures about 30°, twisted from the native s-*trans* configuration, a larger overall twist than for the C_6–C_7 bond.

(B) 4-Methyl Modification. Simulations R2A and R2B modeled the effect of substitutions at the C_4 position of retinal with a methyl group and resulted in structures bR_{R2A} and bR_{R2B}. Attachment to the α-position was studied in simulation R2A, attachment to the β-position in simulation R2B. The results of these calculations are summarized in Figure 9. In bR_{R2A}, retinal maintains its s-*trans* conformation along the polyene skeleton, but many of the dihedral angles show significant twists. The torsion about the C_8–C_9 bond is about 20°, and the C_{12}–C_{13} single bond rotates by about 30° from the native conformation. Most significantly, retinal twists by over 45° about the C_6–C_7 single bond, such that this bond is twisted by 60° from s-*trans*. Retinal in bR_{R2A} has a very twisted form, with the ring region in particular twisted relative to the plane of the membrane (offset somewhat by opposite rotations about the C_6–C_7 and C_{12}–C_{13} bonds). In bR_{R2B}, the system stays very close to the bR_{568} conformation, with only slight rotations about the C_6–C_7 and C_{12}–C_{13} bonds.

(C) 2-Methyl Modification. Simulations R3A and R3B modeled the effect of substitutions at the C_2 position of the

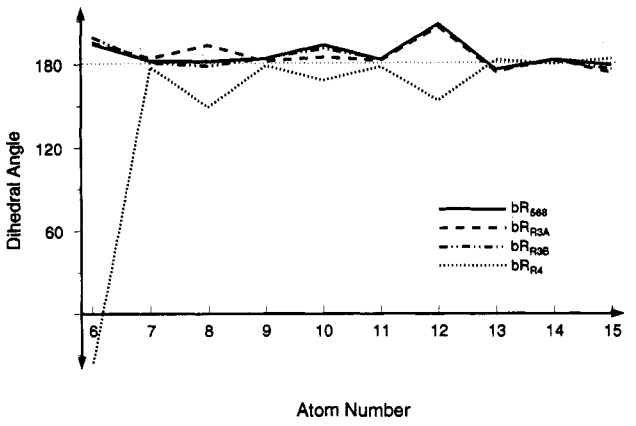

FIGURE 10: Comparison of dihedral angles along retinal backbone, for substitutions at the C_2 position and for the cleaved-ring analogue.

retinal ring with a methyl group and resulted in structures bR_{R3A} and bR_{R3B}. As for the previous analogues, R3A modeled the attachment to the α-position, and R3B to the β-position. Figure 10 summarizes the results of these calculations. For both analogues, there is very little change with respect to the native pigment. bR_{R3A}, in particular, has a retinal conformation essentially identical to that of bR_{568}; bR_{R3B} contains only two significant changes, one being a 15° twist about the C_8–C_9 bond, away from the equilibrium angle,[2] and the other being a 10° relaxation about the C_{10}–C_{11} bond toward the equilibrium angle. In effect, these two counter-rotations in bR_{R3B} leave the retinal ring position and orientation basically unchanged.

(D) Ring Cleavage Modification. Simulation R4, resulting in structure bR_{R4}, was carried out to simulate the effect of cleaving the ring between the 3- and 4-carbons and between the 1- and 6-carbons. Experiments with a cleaved-ring retinal analogue indicate that the absorption maximum is blue-shifted (Sheves *et al.*, 1986). The results for structure bR_{R4} are summarized in Figure 10. This analogue changes considerably with respect to the native pigment; the chromophore twists about every single bond along the retinal chain except the C_{14}–C_{15} bond which has a higher torsional barrier than the other single bonds (see Table 1). The analogue rotated from s-*trans* to s-*cis* about the C_6–C_7 bond, resulting in the terminal ring fragment moving toward the extracellular side. Our simulations suggest that the region into which these atoms move is occupied, in the case of native retinal, by the constituents of the β-ionone ring. The retinal analogue also exhibits a strong overall twist but in an orientation opposite to that of bR_{568}. The dihedral angles of the native pigment which deviate from their equilibrium values are all larger than 180°, while the dihedral angles of bR_{R4} rotate to angles less than 180°. This results in a retinal with a chirality opposite to that of bR_{568}.

DISCUSSION

Simulations G1–G3 provided a refined structure of bR_{568} which is in much closer agreement with the Henderson *et al.* (1990) structure than the structure suggested in Nonella *et al.* (1991) and Zhou *et al.* (1993) as judged by the RMSD values. Simulations R1A,B–R4 modeled artificial pigments in an attempt to judge the validity of the bR_{568} structure and to interpret the observed spectral shifts of retinal analogues.

[2] Equilibrium angles define here the minima of the respective torsional potentials, not the angles for the whole protein in equilibrium.

Refinement of bR_{568}. A distinctive feature of the final structure of bR_{568} determined in simulation G2 is a corkscrew twist in the retinal backbone, due to rotations about the single bonds. Retinal also exhibits a slight curvature along the polyene chain. This curvature did not emerge in the previous refinements of bR (Nonella *et al.*, 1991; Zhou *et al.*, 1993). Circular dichroism (CD) experiments on bR have shown that in the trimeric form of bR in the membrane the CD spectrum is characterized by separated negative and positive bands, whereas the monomeric form is characterized by only one positive band. The trimeric spectrum was interpreted as due to exciton coupling (Heyn *et al.*, 1975; Ebrey *et al.*, 1977; Kriebel & Albrecht, 1977). Recently it has been suggested that the CD spectrum originated from rotations around single C–C bonds along retinal's backbone, which would break the planar symmetry and provide an angular component to π-electron motion (El-Sayed *et al.*, 1989).

Solid-state ^{2}H-NMR studies of retinal in bR also indicate a twisted retinal and suggest the retinal backbone to be curved, bending toward the extracellular side (Ulrich *et al.*, 1992). Table 3 compares the experimentally determined tilt angle θ of retinal methyl groups C_{18}, C_{19}, and C_{20} to the angles for the simulated bR_{568}. These angles compare quite well, with the largest difference seen for C_{18}, which is the methyl group attached to the retinal ring. The experiments were not able to determine the twist angle ϕ, which determines the orientation of the tilted methyl group; in bR_{568}, the methyls C_{18} and C_{19} are twisted to one side of the membrane normal, with the C_{20} methyl twisted to the other side. It is possible that retinal is capable of twisting in either direction, which has been suggested as an explanation for an observed biphasic band in the CD spectrum of bR (Wu & El-Sayed, 1991).

In the simulated structure the retinal ring is found at an angle of about 20° relative to the plane of the Schiff base moiety, this orientation being due to the cumulative effect of several rotations about the single C–C backbone bonds, the twist about the C_6–C_7 bond being very small, such that retinal is in a 6-s-*trans* conformation as previously suggested (Harbison *et al.*, 1985). FTIR linear dichroism and photoselection measurements combined with quantum-chemical calculations have indicated twists around the retinal single bonds (Fahmy *et al.*, 1989). Slight rotations about these single bonds should not affect considerably the absorption maximum and the opsin shift induced by a reduction of the C_6–C_7 torsional angle (Albeck *et al.*, 1992).

The Lys-216 dihedral angles are also seen to be slightly twisted in this structure from their equilibrium positions, by almost 20° in the case of the Schiff base N – C_ϵ bond, to 5° or 10° for the remaining Lys-216 bonds C_ϵ – C_δ, etc. Experimental studies have indicated an unusual coupling between the 15-H rock vibrations and the backbone vibrations of the lysine. This unusual coupling might be associated with a twisted lysine conformation (Gat *et al.*, 1992).

Many recent reports have indicated an important role for water in the structure and function of bR. Vibrational (Doukas *et al.*, 1981; Hildebrandt & Stockburger, 1984) and NMR (de Groot *et al.*, 1989) studies have suggested the presence of bound water within the retinal binding site, and the possibility has been suggested that water molecules participate in proton transfer from Asp-96 to the Schiff base (Henderson *et al.*, 1990; Cao *et al.*, 1991). It was also suggested that water plays an important role in maintaining the high pK_a of the Schiff base and the low pK_a of Asp-85 in the native pigment (Baasov & Sheves, 1986; Gat & Sheves, 1993). Sixteen water molecules, placed within the refined bR_{568} structure, maintain

positions within the protein in three distinct regions: below the Schiff base toward the extracellular side, toward the cytoplasmic side between the Schiff base and Asp-96, and in the region of the Schiff base. The latter water molecules form a complex network of hydrogen bonds within the binding site. Vibrational spectroscopy studies of threonine mutants of bR have suggested the possibility of a "proton wire" connection from Thr-89 to Asp-212, which is formed in the simulated bR_{568} by three water molecules connecting these two residues (Rothschild *et al.*, 1992).

It is currently believed that a major contribution to the opsin shift in bR is a weak Schiff base–counterion electrostatic interaction. Water molecules within the binding site bridge the Schiff base linkage and its negatively charged carboxylate neighbors and, according to our simulations, maintain a relatively large distance between the Schiff base and residues Asp-85 and Asp-212, namely, 6.0 and 4.6 Å, respectively. The distances are considerably larger than the respective distances of 4.1 and 3.7 Å in the EM structure of bR (Henderson *et al.*, 1990). The large distances are in keeping with a weak electrostatic interaction which contributes to the opsin shift (Schulten *et al.*, 1980). In our refined structure, there is no direct interaction between the Schiff base and the aspartic acids; simulations without water, however, have all resulted in Asp-85 and Asp-212 remaining very close to the Schiff base, i.e., at distances similar to those of the EM structure (Henderson *et al.*, 1990). Experiments with dehydrated bR have resulted in a blue-shifted absorption maximum (Hildebrandt & Stockburger, 1984; Papadopolous *et al.*, 1990; Renthal & Regalado, 1991), which could be the result of removal of at least part of the water molecules in the vicinity of the Schiff base, and of a corresponding attraction of Asp-85 and Asp-212 toward the Schiff base. The Schiff base is also seen to form only one hydrogen bond, which is relatively weak due to the fact that the hydrogen bond is not linear, with an angle of about 30°. Accumulated evidence from resonance Raman spectroscopy and FTIR of both bR and model compounds (Aton *et al.*, 1980; Kakitani *et al.*, 1983; Baasov *et al.*, 1987) indicated a weak hydrogen bond between the Schiff base linkage and its environment. The present simulations suggest that this weak hydrogen bond is not between the Schiff base and the counterions Asp-85 or Asp-212 but rather between the Schiff base proton and water. We note that recent model compound studies (Livnah & Sheves, 1993) have suggested that a weak electrostatic interaction between retinal and its counterion prevails also in bovine rhodopsin; however, in this system the Schiff base proton maintains a strong hydrogen bond with its environment. Thus, there is no direct correlation between the Schiff base–counterion electrostatic interactions and the strength of hydrogen bonding to the Schiff base proton.

The counterion residues Asp-85 and Asp-212 differ in their orientation and environment in the structure presented here. Both oxygens of the Asp-85 carboxylate are equidistant from the Schiff base, while one of the oxygens of the Asp-212 carboxylate is significantly closer to the Schiff base than the other. Asp-212 also participates in more hydrogen bonds than Asp-85, due to a larger number of closely adjacent groups. These groups provide a very effective screen for Asp-212, which could possibly explain why Asp-212 interacts electrostatically weakly with the retinal positive charge. Model compound studies have indicated that strong hydrogen bonding to the counterion induces red shifts in the absorption maximum of the retinal protonated Schiff base due to a diminished interaction between the retinal positive charge and the negatively charged counterion (Baasov & Sheves, 1986; Albeck *et al.*, 1992). Replacement of Asp-212 by asparagine did not affect significantly the absorption maximum of retinal, in contrast to Asp-85 replacement, which induced a red shift in the absorption maximum (Needleman *et al.*, 1991; Metz *et al.*, 1992). The difference in Asp-212 and Asp-85 environments may also account for their different behavior in M_{412} formation following light absorption, provided that the differences are also reflected in the L and M intermediates. It was found that Asp-85, and not Asp-212, serves as the proton acceptor in bR's pump cycle. The hydrogen bonding of Asp-212 with the neighboring protein residues may stabilize the negative charge on Asp-212, reducing its pK_a and preventing a proton transfer from the retinal Schiff base to Asp-212. In contrast, the negative charge on Asp-85 is stabilized only by water that forms a bridge between the protonated Schiff base linkage and Asp-85. Following light absorption this structure might be perturbed, and the ΔpK_a between Asp-85 and the Schiff base will be decreased to induce the proton transfer observed between these two groups.

The water structure and unusual helix G conformation above the Schiff base in the simulated structure (toward the cytoplasmic side) suggest one possible means for establishment of a network for transfer of a proton to the Schiff base from Asp-96. In M, it has been observed that the lysine carbonyl adopts an unusually low amide I frequency, which may be the result of hydrogen bonding to water (Takei *et al.*, 1994). In our simulated bR_{568} structure, a water molecule is bound to the lysine carbonyl. This unusual structure may allow, following light absorption and a further perturbation in the lysine backbone structure, the formation of a new water arrangement involving the lysine carbonyl and possibly Asp-96 as well as other residues to account for the low amide I lysine frequency observed in M. From test simulations with two or three of the water molecules in this region removed, the helix G distortion does not seem to be a result of the particular placement of water molecules used. Two Gly residues in this region of helix G (218 and 220) may provide some extra flexibility for the helix to maintain its unusual conformation.

Retinal Analogue Simulations. Retinal analogues modeled in simulations R1A,B–R4 were used to test our refined bR_{568} structure in the vicinity of the retinal ring and to explain some of the structural rearrangements which accommodate artificial pigment experiments. It has been observed that the absorption maximum of bR is very sensitive to substitution at the C_4 position of the retinal ring but relatively insensitive to substitutions at the C_2 position. Substitution of a methyl group at the C_4 position resulted in two photoactive pigments, which absorbed at 550 and 460 nm, each with its own photocycle. Substitution of the bulkier dimethylamino group at the C_4 position resulted in a single pigment absorbing at 460 nm (Sheves *et al.*, 1984). In contrast, substitution of a methyl group at the C_2 position did not significantly affect the absorption maximum.

Both C_2 and C_4 positions of retinal are achiral; however, after incorporation into the protein binding site the two enantiomers are different and chiral discrimination by the protein is possible. It was previously suggested (Sen *et al.*, 1982) that only one enantiomer at the C_4 position was bound to bovine opsin. In the present simulations we investigate the possibility of pigment formation for both enantiomers. For substitution of a methyl at the C_4 position, one possible explanation for the two observed pigments is that each pigment consists of a different enantiomer. The fact that bR_{R2A}

contains very large rotations about retinal's single bonds, particularly about the C_6–C_7 bond, suggest that the respective enantiomer corresponds to the strongly blue-shifted 460-nm peak. bR_{R2B} shows very little conformational change from the native pigment and suggests that the corresponding enantiomer produces the 550-nm peak. Trp-138, which is in very close proximity to the α-position of the 4-carbon (3.6 Å from the $C_{\delta 1}$ atom of Trp-138 to the α hydrogen of C_4), could account for this effect, in that substitution at the α-position results in a steric hindrance which causes a twist in retinal, while substitution at the β-position does not lead to strong steric interactions. For the addition of a larger dimethylamino group to the C_4 position, a similar explanation is suggested. bR_{R1B}, with this substitution at the β-position, resulted in a highly twisted retinal which could explain the blue-shifted 460-nm peak. The very dramatic double-bond rotation observed for bR_{R1A} could indicate that binding of the dimethylamino group to the α-position requires a very large conformational change, perhaps too large to allow this chromophore to constitute with bacterioopsin. The proximity of Trp-138 prevents attachment of the bulky dimethylamino group to the α-position, but this group can be accommodated at the β-position at the price of some twists in retinal.

Simulations of chromophores with a methyl group at the C_2 position produce no significant change in the bR structure, which compares very well with the unshifted spectra observed for these analogues.

In simulations R1A,B–R3A,B, the structure in the vicinity of the Schiff base has been examined for changes induced by retinal modifications. In the six simulations, no major conformational changes have been observed: Asp-85 and Asp-212 maintain their relative distances from the Schiff base, the network of hydrogen-bonded water molecules is maintained, and the overall structure of the residues surrounding the binding site is the same. Experiments have shown, in fact, that the C=N stretching frequency does not change for substitutions at the C_4 position. Simulations R1A,B–R3A,B also support the direction of the methyl groups of retinal, which are oriented in our simulations toward the cytoplasmic side of the membrane. Orientation of these methyl groups toward the extracellular side would reverse the roles of the C_2 and C_4 positions.

In simulation R4 of a linear chromophore (see Figure 8), retinal developed twists about all of its single bonds except the C_{14}–C_{15} bond and, in particular, isomerized to a twisted 6-s-*cis* conformation. This conformation resembles the conformation of the protonated Schiff base of retinal in solution, the latter compound absorbing at 440 nm. Our simulation could explain the observed blue shift (relative to bR_{568}) for this retinal analogue to 532 nm, which is red-shifted relative to the absorption maximum of 440 nm in solution due to the protein maintaining other interactions contributing to the opsin shift, such as the weak electrostatic interactions between the Schiff base linkage and the counterion (in solution the counterion is very close to the protonated Schiff base). This could also shed light on a factor responsible for the chromophore existing in a 6-s-*trans* conformation once bound within the apoprotein—with the β-ionone ring intact, the surrounding residues require a 6-s-*trans* state; however, if this ring is removed, retinal acquires the freedom to adopt the preferred 6-s-*cis* state.

CONCLUSIONS

A cardinal feature of the refined bR_{568} structure is its close agreement with the EM model of bR (Henderson *et al.*, 1990). The RMSD for the C_α backbone atoms comparing the membrane-spanning part of the two structures is 1.8 Å, which is significantly less than the RMSD value of 2.8 Å for the structure reported in Nonella *et al.* (1991), *i.e.*, refined with a protocol which did not include water, explicit hydrogens, and a D helix at the new position. The new RMSD value of 1.8 Å is well within the range of RMSD values arising for structurally well-resolved proteins. Typical RMSD values comparing crystal structures and molecular dynamics simulations for backbone atoms are in the range of 1.5–3.0 Å, deviations of about 2.5 Å being common. A simulation of the L7/L12 ribosomal protein (CTF) in solution compared to its crystal structure yielded particularly small deviations of 1.05 Å (C_α) and 1.63 Å (all atoms) (Daggett & Levitt, 1991). While larger than the latter example, our small RMSD value indicates that our structure fits well with the EM model of bR and that water placed within the protein interior does not cause major structural rearrangements. The small RMSD value encourages further simulation studies since the low value implies that bR, as modeled by molecular dynamics, is structurally stable even though it was here modeled in vacuum rather than in a membrane. The water molecules that were added to the simulated binding site seem to play an important role in the structure. However, although the simulated structure is consistent with spectroscopic and experimental data, one should consider it as only one of many possible choices. Particularly, the number of water molecules is uncertain.

What can we learn from the simulated bR_{568} structure about the protein's function? Obviously, a key element to an eventual answer will be the interactions in retinal's binding site. In this respect the qualitative agreement of our simulations of retinal analogues with respective observations indicates that the present structure reproduces the ring region of the binding site well. We have not described above our many failed retinal analogue simulations which arose with the simulated structures in Nonella *et al.* (1991) and Zhou *et al.* (1993) or with descriptions which do not include hydrogens explicitly. The latter implies that structural detail at a high resolution in the 1-Å range is properly represented in the ring region for the present structure.

Even more essential than the ring region is the Schiff base region of the binding site. The respective structural features constitute certainly the most conspicuous, but also the most daring, features of the refined bR_{568} structure. In agreement with the structure in Zhou *et al.* (1993) it is predicted that the most proximate groups to the Schiff base of retinal are water molecules. The generally held notion that the interactions of the Schiff base and the protein are dominated by Asp-85 and Asp-212 needs to be revised: the counterion of retinal is a hydrogen-bonded complex (de Groot *et al.*, 1989) which involves several water molecules, Asp-212, Asp-85, Tyr-57, Tyr-185, Arg-82, and Thr-89. The water molecules prevent Asp-85 and Asp-212 from approaching the Schiff base hydrogen and forming direct hydrogen bonds. Simulations of the primary photoreaction have revealed (Zhou *et al.*, 1993; Humphrey *et al.*, manuscript in preparation) that the interactions between the counterion complex and the protonated Schiff base in the native case at $T = 300$ K force the nitrogen–proton bond of the Schiff base to point toward the counterion, leaving retinal in a strained conformation, relieved only after the proton is transferred to the counterion complex. The role of the counterion–retinal interactions is also borne out by the observation that an Asp-85 to Asn-85 (Song *et al.*,

1993) mutation apparently extends the lifetime of the excited state of bR_{568} by a factor of 20.

The counterion structure is functionally significant since it determines the spectrum of the pigment, the ΔpK_a value between the Schiff base and the acceptor group Asp-85, and the proton transfer path between the Schiff base and Asp-85. The spectral shifts of retinal during the pump cycle indicate that the counterion complex is altered during the pump cycle, e.g., upon photoisomerization, making the transfer path between the Schiff base and Asp-85 more favorable than the path to Asp-212. The preliminary nature of the counterion structure as presented in this paper is more than offset by the evident fact that only structural details beyond that provided in Henderson *et al.* (1990) can explain the mechanism of bR. Obviously, water will affect protein–retinal interactions and proton pathways; such water requires much higher resolution than is presently in sight. In the case that water is mobile in the protein, it might not be resolved at all. Models of bR which include water are a necessity for interpreting the properties of bR; the present work has outlined refinement procedures which yield such models.

Another essential region of bR_{568} is the space between the retinal Schiff base and the proton-donating side group Asp-96. This region provides the setting for the switching processes subsumed under the so-called M intermediate of the pump cycle. M formation is linked to proton transfer from retinal to a group connected with the extracellular side; M decays when a proton is transfered from a group in contact with the cytoplasmic side to retinal. One expects that retinal, through conformational transitions (*e.g.*, reorienting its proton binding position from pointing in the direction of the extracellular side to the direction of the cytoplasmic side) cooperates with the protein in carrying out the switching processes. In this respect two details of the refined structure are of interest. First, the unusual conformation of the G helix: This helix becomes more ordered in the M state, as observed by Subramaniam *et al.* (1993). Second, three water molecules which bridge the 12-Å distance between retinal and Asp-96 in the modeled structure could actively participate in the processes called the M intermediate; the three or possibly more water molecules, as suggested in Henderson *et al.* (1990), can participate in the transfer of a proton from Asp-96 to retinal. One would expect, therefore, that an interpretation of the key M intermediate of bR's proton pump cycle requires a model of bR which includes water.

Obviously, it would be most desirable to have available structures of bR and of key intermediates of its pump cycle at a resolution which reveals all waters and essential conformational transitions, unfolding, thereby, the mechanism of bacteriorhodospin. Unfortunately, bR as a membrane protein presently defies structure determination at high resolution, while its function as a proton pump may rely on minute structural detail. A possible approach to this dilemma is based on molecular dynamics calculations that demand simulations which start with bR structures refined through addition of water as provided in the present work. There are several avenues for such simulations. First, the refined structure can be employed to evaluate the electronic absorption spectrum of bR, of its mutants, of bR reconstituted with retinal analogues, and of bR's pump cycle intermediates. Second, a renewed attempt of interpreting vibrational spectroscopy of bR can be launched [for earlier attempts see Grossjean *et al.* (1990), Doig *et al.* (1991), and Pollard *et al.* (1992)]. Third, the structure provided can be employed to evaluate the pK_a values relevant for the pump cycle; such evaluation for an unrefined, water-free structure has been provided in Bashford and Gerwert (1992), but it is expected that water present in the protein will affect pK_a values strongly (Gat & Sheves, 1993; B. Honig, private communication). Finally, one should again embark on the efforts started in Nonella *et al.* (1991) and Zhou *et al.* (1993) to describe the pump cycle of bR and of its mutants.

ACKNOWLEDGMENT

We thank Feng Zhou for helpful advice in the refinement simulations carried out here. We thank Prof. R. Henderson for reading the manuscript and for helpful suggestions. The research was carried out at the Resource for Concurrent Biological Computing at the University of Illinois, funded by the National Institutes of Health (Grant P41RR05969), and the majority of simulations were done using Silicon Graphics and Hewlett-Packard workstations operated by the Resource. Some simulations were accomplished on a Cray 2 computer operated by the National Center for Supercomputing Applications funded by the National Science Foundation. M.S. gratefully acknowledges support from the U.S.–Israel Science Foundation and from Beckman and Miller fellowships. W.H. is very grateful for the support of a Computational Science Graduate Fellowship from the U.S. Department of Energy.

REFERENCES

Albeck, A., Livnah, N., Gottlieb, H., & Sheves, M. (1992) *J. Am. Chem. Soc. 114*, 2400–2411.

Aton, B., Doukas, A. G., Narva, D., Callender, R., & Dinur, U. (1980) *Biophys. J. 29*, 79–84.

Baasov, T., & Sheves, M. (1986) *Biochemistry 25*, 5249–5258.

Baasov, T., Friedmann, N., & Sheves, M. (1987) *Biochemistry 26*, 3210–3217.

Bashford, D., & Gerwert, K. (1992) *J. Mol. Biol. 224*, 473–486.

Birge, R. R. (1990) *Annu. Rev. Phys. Chem. 41*, 683–733.

Birge, R. R., Murray, L. P., Zidovetzki, R., & Knapp, H. M. (1987) *J. Am. Chem. Soc. 109*, 2090–2101.

Braiman, M. S., Mogi, T., Marti, T., Stern, L. J., Khorana, H. G., & Rothschild, K. J. (1988) *Biochemistry 27*, 8516–8520.

Brooks, B. R., Bruccoleri, R. E., Olafson, B. D., States, D. J., Swaminathan, S., & Karplus, M. (1983) *J. Comput. Chem. 4* (2), 187–217.

Brünger, A. T. (1988) *X-PLOR*, The Howard Hughes Medical Institute and Department of Molecular Biophysics and Biochemistry, Yale University, New Haven, CT.

Brünger, A., Schulten, Z., & Schulten, K. (1983) *Z. Phys. Chem. NF136*, 1–63.

Cao, Y., Váró, G., Chang, M., Ni, B., Needleman, R., & Lanyi, J. K. (1991) *Biochemistry 30*, 10972–10979.

Carlacci, L., Schulz, M. W., & Chou, K. C. (1991) *Protein Eng. 4*, 885–889.

Daggett, V. & Levitt, M. (1991) *Chem. Phys. 158*, 501–512.

Dancshazy, Z., Ebrey, T. G., & Govindjee, R. (1988) *Proc. Natl. Acad. Sci. U.S.A. 85*, 6358–6361.

de Groot, H. J. M., Harbison, G. S., Herzfeld, J., & Griffin, R. G. (1989) *Biochemistry 28*, 3346–3353.

Doig, S. J., Reid, P. J., & Mathies, R. A. (1991) *J. Phys. Chem. 95*, 6372–6379.

Doukas, A., Pandi, A., Suzuki, T., Callender, R., & Ottolenghi, M. (1981) *Biophys. J. 33*, 275–278.

Dupuis, P., Harosi, F., Sandorfy, C., Leclercq, J. M., & Vocelle, D. (1980) *Rev. Can. Biol., 39*, 247–258.

Earnest, T. N., Roepe, P., Braiman, M. S., Gillespie, J., & Rothschild, K. J. (1986) *Biochemistry 25*, 7793–7798.

Ebrey, T. (1993) in *Thermodynamics of Membranes, Receptors and Channels* (Jacobson, M., Ed.) pp 353–387, CRC Press, Boca Raton, FL.

Ebrey, T. G., Becher, B., Mao, B., Kilbride, P., & Honig, B. (1977) *J. Mol. Biol. 112*, 377–397.
El-Sayed, M. A., Lin, C. T., & Mason, W. R. (1989) *Proc. Natl. Acad. Sci. U.S.A. 86*, 5376–5379.
Engelhard, M., Hess, B., Metz, G., Kreutz, W., Siebert, F., Soppa, J., & Oesterhelt, D. (1990) *Eur. Biophys. J. 18*, 17–24.
Fahmy, K., Siebert, F., Grossjean, M., & Tavan, P. (1989) *J. Mol. Struct. 214*, 257–288.
Gat, Y., & Sheves, M. (1993) *J. Am. Chem. Soc. 115*, 3772.
Gat, Y., Grossjean, M., Pinevsky, I., Takei, H., Rothman, Z., Sigrist, H., Lewis, A., & Sheves, M. (1992) *Proc. Natl. Acad. Sci. U.S.A. 89*, 2434–2438.
Gerwert, K. & Siebert, F. (1986) *EMBO J. 4*, 805–812.
Gerwert, K., Hess, B., Soppa, J., & Oesterhelt, D. (1989). *Proc. Natl. Acad. Sci. U.S.A. 86*, 4943–4947.
Grossjean, M. F., Tavan, P., & Schulten, K. (1990) *J. Phys. Chem. 94*, 8059–8069.
Harbison, G. S., Smith, S. O., Pardoen, J. A., Courtin, J. M. L., Lugtenburg, J., Herzfeld, J., Mathies, R. A., & Griffin, R. G. (1985) *Biochemistry 24*, 6955–6962.
Henderson, R., Baldwin, J. M., Ceska, T. A., Zemlin, F., Beckmann, E., & Downing, K. H. (1990) *J. Mol. Biol. 213*, 899–929.
Heyn, M. P., Bauer, P. J., & Dencher, N. A. (1975) *Biochem. Biophys. Res. Commun. 67*, 897–903.
Heyn, M. P., Westerhausen, J., Wallat, I., & Seiff, F. (1988) *Proc. Natl. Acad. Sci. U.S.A. 85*, 2146–2150.
Hildebrandt, P., & Stockburger, M. (1984) *Biochemistry 23*, 5539–5548.
Jorgensen, W. L., Chandrasekhar, J., Madura, J. D., Impey, R. W., & Klein, M. L. (1983) *J. Chem. Phys. 79*, 926–935.
Kakitani, T., Kakitani, H., Rodman, H., Honig, B., & Callender, R. (1983) *J. Phys. Chem. 87*, 3620–3628.
Khorana, H. G. (1988) *J. Biol. Chem. 263*, 7439–7442.
Kouyama, T., Kouyama, A. M., Ikegami, A., Mathew, M. K., & Stoeckenius, W. (1988) *Biochemistry 27*, 5855–5863.
Kraulis, P. (1991) *J. Appl. Crystallogr. 24*, 946–950.
Kriebel, A., & Albrecht, A. (1977) *J. Chem. Phys. 65*, 4575–4583.
Lanyi, J. K. (1992) *J. Bioenerg. Biomembr. 24*, 169–179.
Lin, S. W., & Mathies, R. A. (1989) *Biophys. J. 56*, 653–660.
Livnah, N., & Sheves, M. (1993) *J. Am. Chem. Soc. 115*, 351.
Lozier, R. H., Niederberger, W., Ottolenghi, M., Sivorinovsky, G., & Stoechenius, J. W. (1978) in *Energetics and Structure of Halophilic Microorganisms* (Caplan, S. R. J., & Ginzburg, M., Eds.) pp 123–141. North Holland Biomedical Press/ Elsevier, Amsterdam.
Maeda, A., Sasaki, J., Shishida, Y., & Yoshizawa, T. (1992) *Biochemistry 31*, 462–467.
Mathies, R. A., Lin, S. W., Ames, J. B., & Pollard, W. T. (1991) *Annu. Rev. Biochem. Bioeng. 20*, 491–518.
Metz, G., Siebert, F., & Engelhard, M. (1992) *FEBS Lett. 303*, 237.
Mogi, T., Marti, T., & Khorana, H. G. (1989a) *J. Biol. Chem. 264*, 14197–14201.
Mogi, T., Stern, L. J., Chao, B. H., & Khorana, H. G. (1989b) *J. Biol. Chem. 264*, 14192–14196.
Nagle, J. F., & Mille, M. (1981) *J. Chem. Phys. 74*, 1367–1372.
Nakanishi, K., Arnaboldi, M., Baloghnair, V., & Honig, B. (1980) *J. Am. Chem. Soc. 102*, 7945–7947.
Needleman, R., Chang, M., Ni, B., Varo, G., Fornes, J., White, S. H., & Lanyi, J. K. (1991) *J. Biol. Chem. 266*, 11478–11484.
Nonella, M., Windemuth, A., & Schulten, K. (1991) *J. Photochem. Photobiol. 54* (6), 937–948.
Oesterhelt, D., Tittor, J., & Bamberg, E. (1992) *J. Bioenerg. Biomembr. 24*, 181–191.
Orlandi, G., & Schulten, K. (1979) *Chem. Phys. Lett. 64*, 370–374.
Ottolenghi, M., & Sheves, M. (1989) *J. Membr. Biol. 112*, 193–212.
Papadopoulos, G., Dencher, N., Zaccai, G., & Büldt, G. (1990) *J. Mol. Biol. 214*, 15–19.
Pollard, W. T., Dexheimer, S. L., Wang, Q., Peteanu, L. A., Shank, C. V., & Mathies, R. A. (1992) *J. Phys. Chem. 96*, 6147–6158.
Polygen Corp. (1988) *Quarita*, 200 Fifth Ave, Waltham, MA.
Renard, M., & Delmelle, M. (1985) *Eur. Biophys. J. 12*, 223–228.
Renthal, R., & Regalado, R. (1992) *Photochem. Photobiol. 54*, 931–935.
Rothschild, K. J., He, Y. W., Sonar, S., Marti, T., & Khorana, H. G. (1992) *J. Biol. Chem. 267*, 1615–1622.
Santarsiero, B. D., & James, M. N. G. (1990) *J. Am. Chem. Soc. 112*, 9416–9418.
Schulten, K., & Tavan, P. (1978) *Nature 272*, 85–86.
Schulten, K., Dinur, U., & Honig, B. (1980) *J. Chem. Phys. 73* (8), 3927–3935.
Schulten, K., Schulten, Z., & Tavan, P. (1984) in *Information and Energy Transduction in Biological Membranes* (Bolis, L., Helmreich, E. J. M., & Passow, H., Eds.) pp 113–131, Alan R. Liss, Inc., New York.
Sen, R., Carriker, J., Balogh-Nair, V., & Nakanishi, K. (1982) *J. Am. Chem. Soc. 104*, 3214–3216.
Sheves, M., Baasov, T., Friedman, N., Ottolenghi, M., Feinmann-Weinberg, R., Rosenbach, V., & Ehrenberg, B. (1984) *J. Am. Chem. Soc. 106*, 2435–2437.
Sheves, M., Albeck, A., Friedman, N., & Ottolenghi, M. (1986) *Proc. Natl. Acad. Sci. U.S.A. 83*, 3262–3266.
Song, L., El-Sayed, M. A., & Lanyi, J. K. (1993) *Science 261*, 891–894.
Stern, L. J., & Khorana, H. G. (1989) *J. Biol. Chem. 264*, 14202–14208.
Subramaniam, S., Gerstein, M., Oesterhelt, D., & Henderson, R. (1993) *EMBO J. 12*, 1–8.
Takei et al. (1994) *J. Biol. Chem.* (in press).
Tavan, P., Schulten, K., & Oesterhelt, D. (1985) *Biophys. J. 47*, 415–430.
Ulrich, A. S., Wallat, I., Heyn, M. P., & Watts, A. (1992) in *Structures and Functions of Retinal Proteins* (Rigaud, J. L., Ed.) Vol. 221, pp 247–249, Colloque INSERM/John Libbey Eurotext Ltd., Montrouge, France.
van der Steen, R., Biesheuvel, P. L., Mathies, P. L., & Lugtenburg, J. (1986) *J. Am. Chem. Soc. 108*, 6410–6411.
Váró, G., & Lanyi, J. K. (1990) *Biochemistry 29*, 6858–6865.
Váró, G., & Lanyi, J. K. (1991a) *Biochemistry 30*, 5008–5015.
Váró, G., & Lanyi, J. K. (1991b) *Biochemistry 30*, 5016–5022.
Wu, S., & El-Sayed, M. A. (1991) *Biophys. J. 60*, 190–197.
Zhou, F., Windemuth, A., & Schulten, K. (1993) *Biochemistry 32* (9), 2291–2306.